

Characterization of cluster/monomer ratio in pulsed supersonic gas jets

X. Gao, X. Wang, B. Shim, A. V. Arefiev, R. Korzekwa, and M. C. Downer^{a)}

Institute for Fusion Studies, University of Texas at Austin, Austin, Texas 78712, USA

(Received 30 August 2011; accepted 23 January 2012; published online 8 February 2012)

We determine cluster mass fraction $f_c(\mathbf{r}, t)$ at position \mathbf{r} within, and time t after firing, a pulsed supersonic gas jet by measuring femtosecond evolution of the jet's refractive index by single-shot frequency domain holography. A fs pump pulse singly ionizes monomers, while quasi-statically ionizing and heating clusters to a level at which recombination remains negligible as clusters expand. Under these conditions, index evolves in two simple steps corresponding to monomer and cluster contributions, allowing recovery of f_c without detailed cluster dynamic modeling. Variations of f_c with t are measured. © 2012 American Institute of Physics. [doi:10.1063/1.3683543]

Interaction of intense laser pulses with atomic clusters has impacted several areas of laser-plasma science,¹ including controlled generation of hot plasma,² energetic neutrons,³ pulsed x-rays,⁴ optical harmonics,⁵ and plasma waveguides,⁶ as well as laser-driven acceleration of electrons⁷ and ions.⁸ These experiments typically use clusters of average radius $\bar{r}_c > 10$ nm (containing $N_{\#} > 10^5$ atoms/cluster) formed by condensation in pulsed supersonic noble gas jets of total atomic density $N_{\text{tot}} \sim 10^{19}$ cm⁻³. Accurate interpretation of these experiments relies on accurate characterization of N_{tot} , \bar{r}_c , and cluster mass fraction $f_c \equiv N_{\#}N_c / (N_m + N_{\#}N_c)$, where N_m and N_c denote the number density of monomers and clusters, respectively. N_{tot} is typically determined by interferometry of the neutral jet, and \bar{r}_c by Rayleigh scatter⁹ and/or estimates based on Hagen's empirical parameter Γ^* .¹⁰ By contrast, no generally accepted method exists for estimating or measuring f_c for jets typical of intense laser experiments, although techniques restricted to lower N_{tot} and \bar{r}_c and/or to molecular gas jets have been reported.¹¹ While $f_c \sim 1.0$ is often assumed,⁹ simulations of cluster formation¹⁶ show $f_c < 0.5$ is typical for room temperature supersonic rare gas jets. Not only is direct knowledge of f_c lacking, but Rayleigh scatter measurements yield an algebraic combination of N_c and \bar{r}_c , and thus rely on an unverified assumption about f_c to extract \bar{r}_c . Thus an *in-situ* method for determining f_c in dense noble gas jets is needed.

Here we determine $f_c(\mathbf{r}, t)$ at position \mathbf{r} within, and time t after firing, a cluster jet by a single-shot, fs-time-resolved, frequency domain holography (FDH) (Ref. 13) measurement of the jet refractive index $n_{\text{jet}}(\mathbf{r}, t; \tau)$. Here τ denotes time delay after a 40 fs, 800 nm, ~ 2 mJ pump pulse ionizes both monomers and clusters. Ionization of monomers (and possibly very small clusters) causes n_{jet} to drop immediately during the pump by an amount proportional to N_m , before large ionized clusters contribute significantly to n_{jet} . The latter begin to contribute after several hundred fs, when their internal electron density drops to the critical density $n_{\text{crit}} = \epsilon_0 m_e \omega_{\text{pr}}^2 / e^2$ of the probe pulse (frequency ω_{pr}) as a result of hydrodynamic expansion. The details of this evolution, however, are not relevant here. The present method

relies only on the asymptotic value of n_{jet} , reached after clusters expand into uniform monomer plasma, causing a second delayed drop in n_{jet} that is proportional to $N_{\#}N_c$. Thus n_{jet} evolves in two steps corresponding to monomer and cluster contributions, allowing recovery of f_c . Since τ is measured in fs and t in ms, the jet may be considered frozen in t throughout the index measurement. In a recent conference proceedings paper,¹⁴ we presented a preliminary measurement of 2-step index evolution using *multi-shot* frequency-domain interferometry, in which $n_{\text{jet}}(\tau)$ for each delay τ is measured on a separate shot. However, shot-to-shot fluctuations of the laser and jet significantly compromised the results. Here, by measuring $n_{\text{jet}}(\tau)$ in a *single* shot, sensitivity to shot-to-shot fluctuations was eliminated. Moreover, the greatly increased measurement speed enables convenient scans of the dependence of f_c on jet parameters (*e.g.*, t , backing pressure, temperature).

In our experiments, a solenoid-controlled valve (General Valve Series 9, opening time 800 μ s, backing pressure 500 psi at RT) controlled a supersonic argon jet emerging from a conical nozzle (750 μ m orifice, 9° half angle, $\Gamma^* \approx 1.3 \times 10^5$) into a 10^{-3} Torr vacuum. Fig. 1 shows the FDH schematic. A 10 Hz train of 800 nm, 40 fs Ti:S laser pulses with 10^6 :1 peak-to-background ratio at 1 ps from the peak (higher at longer times) was split into pump and probe beams. Probe pulses were frequency doubled in a 500 μ m KDP crystal, split by a Michelson interferometer into probe and reference pulses separated by 3 ps, each chirped to ~ 2 ps

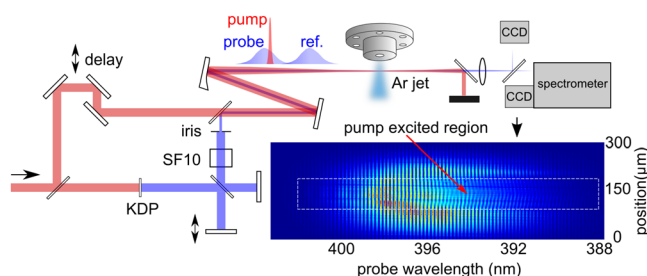


FIG. 1. (Color online) Schematic set-up for single-shot, fs-time-resolved measurement of cluster gas jet refractive index $n_{\text{jet}}(\tau)$. Frequency-domain hologram (lower right) records pump-induced phase alterations imprinted on probe.

^{a)}Electronic mail: downer@physics.utexas.edu.

duration in 2 cm SF10 glass, and irised down to ensure a large focused spot with uniform wavefront. These 400 nm pulses recombined with the 800 nm pump at a dichroic beam splitter, with reference pulse leading and probe spanning delays $-0.75 < \tau < 1.3$ ps. An off-axis parabola focused the 3 co-propagating pulses ($f^\# = 60$ for pump) through an off-center chord of the gas jet about 1 mm from the nozzle where the interaction length was ~ 2 mm (compared to Rayleigh length $z_R = 10$ mm), and probe absorption not too severe. Reference and probe pulses were frequency filtered and relay-imaged from the gas jet exit to the entrance slit of an imaging spectrometer, with the pumped region (monitored by a CCD camera) centered on the slit. They interfered at the spectrometer's detection plane, where a second CCD camera recorded each frequency-domain hologram (see example in Fig. 1). A Fourier transform procedure^{15,16} then reconstructed the pump-induced temporal phase shift $\Delta\phi_{\text{pr}}(\tau)$ of the probe along the pump propagation axis.

The squares in Fig. 2 show $\Delta\phi_{\text{pr}}(\tau)$ from pump-probing the jet at $t = 0.3$ ms, before large clusters formed, in part because total atomic density was still low. $\Delta\phi_{\text{pr}}(\tau)$ drops immediately by ~ 2 rad as monomers (and possibly very small clusters) ionize, then remains nearly constant. The circles show $\Delta\phi_{\text{pr}}(\tau)$ from pump-probing the jet at $t = 0.8$ ms, after clusters had formed. Two components can be identified. The fast component, which coincidentally has the same $\Delta\phi_{\text{pr}}(\tau)$ as the squares, is caused by ionization of monomers. The slow component comes from large expanding clusters, and reaches a steady state at $\tau \sim 1$ ps as clusters approach a uniform underdense plasma.

The probe phase shift is related to refractive index by,

$$\Delta\phi_{\text{pr}} = \frac{2\pi}{\lambda} \int [n_{\text{jet}}(z) - n_{\text{gas}}(z)] dz. \quad (1)$$

where z denotes distance from the gas jet entrance, $n_{\text{gas}}(z) = 1 + N_{\text{tot}}(z)\alpha/2\epsilon_0$ is the jet's refractive index (including both monomers and clusters) before ionization, and α is the atomic polarizability of a free Ar atom, which we assume to be the same for an atom in a cluster (α in solid Ar is only 6% smaller than for free atoms¹⁷). The monomer plasma contribution to $n_{\text{jet}}(z)$ is

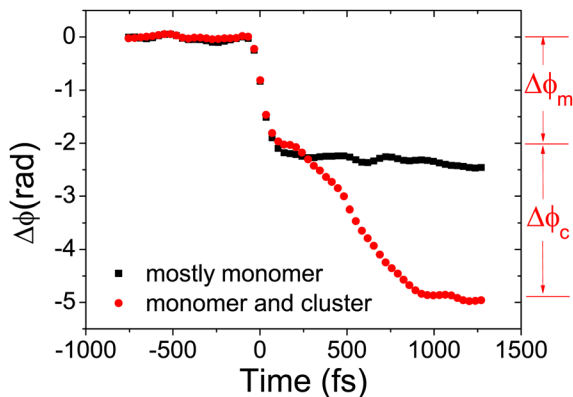


FIG. 2. (Color online) Two fs-time-resolved probe phase shifts $\Delta\phi_{\text{pr}}(\tau)$, each measured in a single shot, at time $t = 0.3$ ms (squares) or 0.8 ms (circles) after opening of gas jet valve.

$$n_m(z) = 1 - \frac{1}{2} \frac{Z_m(1 - f_c(z))N_{\text{tot}}(z)}{n_{\text{crit}}}, \quad (2)$$

where Z_m is the charge state of the monomers, and we have assumed a tenuous plasma ($N_{\text{tot}} \ll n_{\text{crit}}$). The asymptotic cluster contribution to $n_{\text{jet}}(z)$ is an additional term $-Z_c f_c(z)N_{\text{tot}}(z)/2n_{\text{crit}}$, where Z_c is the charge state of the ionized clusters at $\tau > 1$ ps. Here, for simplicity, we assume $f_c(z)$ is constant along the short interaction length. However, it should be straightforward to resolve z -variations by focusing the pump to a Rayleigh length shorter than the jet thickness. With this assumption, the monomer-induced phase shift is

$$\Delta\phi_m = -\frac{\pi}{\lambda} \left[\frac{Z_m(1 - f_c)}{n_{\text{crit}}} + \frac{\alpha}{\epsilon_0} \right] \int N_{\text{tot}}(z) dz \quad (3)$$

for $Z_m \geq 1$. The asymptotic cluster contribution is

$$\Delta\phi_c = -\frac{\pi Z_c f_c}{\lambda n_{\text{crit}}} \int N_{\text{tot}}(z) dz. \quad (4)$$

The cluster fraction f_c is related to the observables $\Delta\phi_m$, $\Delta\phi_c$ by

$$f_c = \frac{(Z_m + \alpha n_{\text{crit}}/\epsilon_0)\Delta\phi_c}{Z_c \Delta\phi_m + Z_m \Delta\phi_c}. \quad (5)$$

This result is independent of the integrated density profile, which therefore need not be characterized. In this sense, the method is self-referencing.

Evaluation of Eq. (5) requires knowledge of Z_m and Z_c . Z_m was calculated from the Ammosov-Delone-Krainov (ADK) formula.¹⁸ The dependence of Z_m on I_{pu} is plotted in Fig. 3 (squares). By choosing $I_{\text{pu}} = 4.0 \times 10^{14}$ W/cm² in the $Z_m = 1$ plateau between the 1st and 2nd ionization thresholds, we minimize sensitivity of the result to small uncertainty in I_{pu} . This intensity was confirmed *in-situ* by varying pump energy and observing the appearance of monomer ionization. For hydrogen cluster, Z_c can be determined without uncertainty by choosing I_{pu} at which the cluster is fully ionized. For Ar cluster irradiated at moderate intensity, calculation of Z_c ($\tau \sim 1$ ps) would in general require an intensive

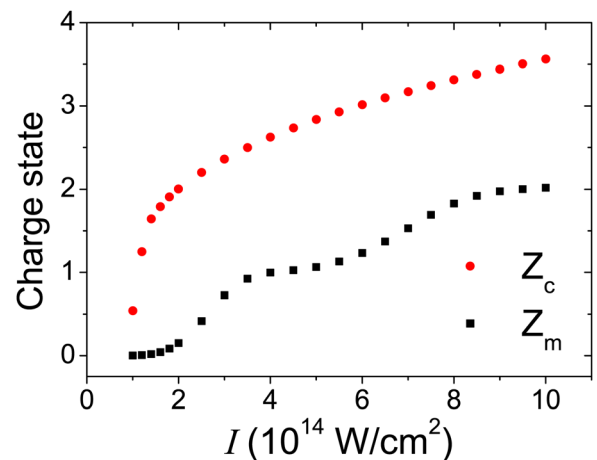


FIG. 3. (Color online) Charge state of Ar cluster (circles) and monomer (squares) vs. pump intensity, calculated from static nanoplasma model of Ref. 2 with modifications (1)–(4) as described in text.

computer simulation of cluster ionization, heating and hydrodynamic expansion.¹⁹ However, at our I_{pu} , recombination during ~ 1 ps of cluster expansion is $<10\%$ estimated by a modified expansion model^{14,20} including recombination, and can be safely neglected. A much simpler modified nanoplasma model² with no expansion then suffices for calculating Z_c . In addition to the elements in Ref. 2, our calculation of cluster heating and ionization included (1) three-body recombination,²¹ (2) the temperature decrease due to the increase in the total number of electrons, (3) the energy loss/gain due to ionization/recombination, and (4) lowering of ionization energy.²² To indicate the sensitivity of the result to assumptions of the model, Table I lists Z_c calculated using the nanoplasma model of Ref. 2 with and without expansion, and with our modifications (1)-(4) without expansion. At our I_{pu} , modification (1) is most important, since electron temperature is <130 eV.²³ The calculation is independent of cluster radius. Nanoplasma model assumptions for given experimental parameters can be validated by comparing measured and calculated fs-time-resolved cluster absorption.^{14,19} The dependence of Z_c on I_{pu} using all modifications is plotted in Fig. 3. For the conditions of the circles in Fig. 2, we find $f_c = 0.42$. Our model assumes that the electron population inside each cluster is a single-temperature Maxwellian. Any hot electrons that can be generated in the cluster, as those discussed in Refs. 24 and 25, are therefore neglected. This approach is justified if the relative fraction of hot electrons is below 10^{-4} , which is the case for the experiments of Refs. 24 and 25. This condition guarantees that the hot electrons are unable to change Z of all the ions from 3 to 4 on a time scale of our measurements (1 ps).

As an example of jet parameter scan, Fig. 4 (main panel) shows $f_c(t)$ vs. time t after the valve opens. Each data point is the average of 20 single-shot measurements of f_c . f_c rises between 0.3 and 0.7 ms, then levels off until 1.0 ms (0.2 ms after the valve closes) before dropping sharply. For comparison, the inset of Fig. 4 shows phase shift through the un-ionized jet measured by transverse interferometry, which is proportional to $N_{\text{tot}}(t)$. While the two curves resemble each other qualitatively, they differ in details. For example, N_{tot} begins dropping after $t = 0.8$ ms, whereas f_c drops only after 1.0 ms. Scans of additional jet parameters will be presented elsewhere. It is worth pointing out that our measurements and the simulations of Ref. 12 show that the majority of atoms are unclustered. A direct quantitative comparison with the results of the model of Ref. 12 would be useful, but it requires a dedicated simulation that uses our nozzle geometry.

TABLE I. Charge state Z_c of cluster at $t = 100$ fs for $I_{\text{pu}} = 4 \times 10^{14}$ W/cm², $\tau = 40$ fs calculated using nanoplasma model of Ref. 2, and with modifications (1)–(4) as described in text, and (2nd row) f_c obtained with $Z_m = 1$ and indicated Z_c .

	Ref. 2 nanoplasma model		Modification			
	w. expansion	w/o expansion	1	1,2	1-3	1-4
Z_c	5.98	6.05	3.18	2.57	2.24	2.62
f_c	0.23	0.23	0.37	0.42	0.46	0.42

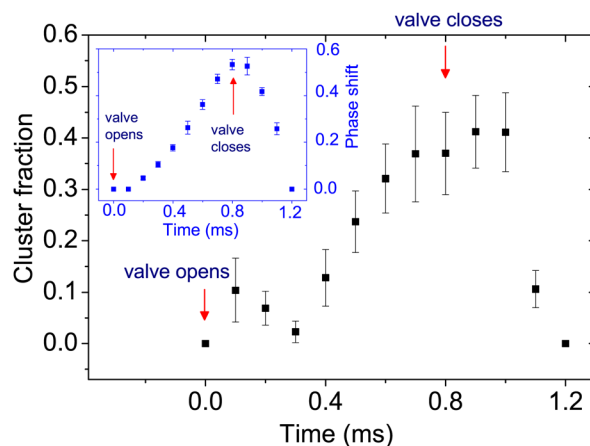


FIG. 4. (Color online) Cluster fraction f_c vs. time t after opening of valve of gas jet. Each error bars indicates the standard deviation of 20 single-shot measurements. Inset: Phase shift from the neutral gas jet (measured by transverse interferometry) vs. t .

In conclusion, we demonstrate an *in-situ* method for determining cluster fraction f_c in atmospheric density gas jets by measuring the jet's fs-time-resolved refractive index in a single shot. Monomers and clusters contribute to the index drop in two sequential steps, which are easily distinguished. The accuracy of f_c depends on the accuracy with which monomer and cluster ionization states can be calculated. The high measurement speed enables convenient scans of f_c dependence on jet parameters.

This work was supported by U.S. NSF Grant PHY-0936283 and DOE Grant DE-FG03-96ER40954. We acknowledge valuable discussions with B. Breizman.

- ¹T. Fennel, K. H. Meiwes-Broer, J. Tiggesbaumer, P. G. Reinhard, P. M. Dinh, and E. Suraud, *Rev. Mod. Phys.* **82**, 1793 (2010).
- ²T. Ditmire, T. Donnelly, A. M. Rubenchik, R. W. Falcone, and M. D. Perry, *Phys. Rev. A* **53**, 3379 (1996).
- ³K. W. Madison, P. K. Patel, D. Price, A. Edens, M. Allen, T. E. Cowan, J. Zweiback, and T. Ditmire, *Phys. Plasmas* **11**, 270 (2004).
- ⁴F. Dorchies, F. Blasco, C. Bonte, T. Caillaud, C. Fourment, and O. Peyrusse, *Phys. Rev. Lett.* **100**, 205002 (2008).
- ⁵B. Shim, G. Hays, R. Zgadzaj, T. Ditmire, and M. C. Downer, *Phys. Rev. Lett.* **98**, 123902 (2007).
- ⁶V. Kumarappan, K. Y. Kim, and H. M. Milchberg, *Phys. Rev. Lett.* **94**, 205004 (2005).
- ⁷Y. Fukuda, Y. Akahane, M. Aoyama, Y. Hayashi, T. Homma, N. Inoue, M. Kando, S. Kanazawa, H. Kiriya, S. Kondo, H. Kotaki, S. Masuda, M. Mori, A. Yamazaki, K. Yamakawa, E. Y. Echkina, I. N. Inovenkov, J. Koga, and S. V. Bulanov, *Phys. Lett. A* **363**, 130 (2007).
- ⁸Y. Fukuda, A. Y. Faenov, M. Tampo, T. A. Pikuz, T. Nakamura, M. Kando, Y. Hayashi, A. Yogo, H. Sakaki, T. Kameshima, A. S. Pirozhkov, K. Ogura, M. Mori, T. Z. Esirkepov, J. Koga, A. S. Boldarev, V. A. Gasilov, A. I. Magunov, T. Yamauchi, R. Kodama, P. R. Bolton, Y. Kato, T. Tajima, H. Daido, and S. V. Bulanov, *Phys. Rev. Lett.* **103**, 165002 (2009).
- ⁹K. Y. Kim, V. Kumarappan, and H. M. Milchberg, *Appl. Phys. Lett.* **83**, 3210 (2003).
- ¹⁰O. F. Hagena, *Rev. Sci. Instrum.* **63**, 2374 (1992).
- ¹¹D. Dreyfuss and H. Y. Wachman, *J. Chem. Phys.* **76**, 2031 (1982); U. Buck and R. Krohne, *ibid.* **105**, 5408 (1996); A. Amirav, U. Even, and J. Jortner, *ibid.* **75**, 2489 (1981); J. Wormer, V. Guzielski, J. Stapelfeldt, and T. Moller, *Chem. Phys. Lett.* **159**, 321 (1989); A. Ramos, J. M. Fernandez, G. Tejeda, and S. Montero, *Phys. Rev. A* **72**, 053204 (2005).
- ¹²A. S. Boldarev, V. A. Gasilov, A. Y. Faenov, Y. Fukuda, and K. Yamakawa, *Rev. Sci. Instrum.* **77**, 083112 (2006).
- ¹³S. P. Le Blanc, E. W. Gaul, N. H. Matlis, A. Rundquist, and M. C. Downer, *Opt. Lett.* **25**, 764 (2000).

- ¹⁴A. V. Arefiev, X. Gao, M. R. Tushentsov, X. Wang, B. Shim, B. N. Breizman, and M. C. Downer, *High Energy Density Phys.* **6**, 121 (2010).
- ¹⁵M. Takeda, H. Ina, and S. Kobayashi, *J. Opt. Soc. Am.* **72**, 156 (1982).
- ¹⁶K. Y. Kim, I. Alexeev, and H. M. Milchberg, *Appl. Phys. Lett.* **81**, 4124 (2002).
- ¹⁷T. H. Keil, *J. Chem. Phys.* **46**, 4404 (1967).
- ¹⁸M. V. Ammosov, N. B. Delone, and V. P. Krainov, *Sov. Phys. JETP* **64**, 1191 (1986).
- ¹⁹H. M. Milchberg, S. J. McNaught, and E. Parra, *Phys. Rev. E* **64**, 056402 (2001).
- ²⁰A. Arefiev, B. Breizman, V. Khudik, X. Gao, and M. Downer, *Plasma Fusion Res.* **5**, S2071 (2010).
- ²¹A. V. Gurevich and L. P. Pitaevskii, *Sov. Phys. JETP* **19**, 870 (1964).
- ²²P. Hilse, M. Moll, M. Schlanges, and T. Bornath, *Laser Phys.* **19**, 428 (2009).
- ²³J. Jha and M. Krishnamurthy, *J. Phys. B: At. Mol. Opt. Phys.* **41**, 041002 (2008).
- ²⁴J. Abdallah, A. Y. Faenov, I. Y. Skobelev, A. I. Magunov, T. A. Pikuz, T. Auguste, P. D'Oliveira, S. Hulin, and P. Monot, *Phys. Rev. A* **63**, 032706 (2001).
- ²⁵M. E. Sherrill, J. Abdallah, J. G. Csanak, E. S. Dodd, A. Y. Faenov, A. I. Magunov, T. A. Pikuz, and I. Y. Skobelev, *Phys. Rev. E* **73**, 066404 (2006).